



Article

# Inhibitory Effectiveness of Gomisin A, a Dibenzocyclooctadiene Lignan Isolated from *Schizandra chinensis*, on the Amplitude and Gating of Voltage-Gated Na<sup>+</sup> Current

Wei-Ting Chang <sup>1,2,3</sup> and Sheng-Nan Wu <sup>4,5,6,\*</sup>

<sup>1</sup> Institute of Clinical Medicine, College of Medicine, National Cheng Kung University, Tainan 70101, Taiwan; cmcvecho2@gmail.com

<sup>2</sup> Chi-Mei Medical Center, Division of Cardiovascular Medicine, Tainan 71004, Taiwan

<sup>3</sup> Department of Biotechnology, Southern Taiwan University of Science and Technology, Tainan 71004, Taiwan

<sup>4</sup> Department of Physiology, National Cheng Kung University Medical College, No. 1, University Road, Tainan 70101, Taiwan

<sup>5</sup> Institute of Basic Medical Sciences, National Cheng Kung University Medical College, Tainan 70101, Taiwan

<sup>6</sup> Department of Medical Research, China Medical University Hospital, China Medical University, Taichung 709, Taiwan

\* Correspondence: cmcvecho@gmail.com; Tel.: +886-6-2353535-5334; Fax: +886-6-2362780

Received: 1 November 2020; Accepted: 19 November 2020; Published: 21 November 2020



**Abstract:** Gomisin A (Gom A), a lignan isolated from *Schizandra chinensis*, has been reported produce numerous biological activities. However, its action on the ionic mechanisms remains largely unanswered. The present experiments were undertaken to investigate the possible perturbations of Gom A or other related compounds on different types of membrane ionic currents in electrically excitable cells (i.e., pituitary GH<sub>3</sub> and pancreatic INS-1 cells). The exposure to Gom A led to the differential inhibition of peak and end-pulse components of voltage-gated Na<sup>+</sup> current ( $I_{Na}$ ) in GH<sub>3</sub> cells with effective IC<sub>50</sub> of 6.2 and 0.73 μM, respectively. The steady-state inactivation curve of  $I_{Na}$  in the presence of Gom A was shifted towards a more hyperpolarized potential. However, neither changes in the overall current-voltage relationship nor those for the gating charge of the current were demonstrated. The application of neither morin (10 μM) nor hesperidin (10 μM) perturbed the strength of  $I_{Na}$ , while sesamine could suppress it. However, in the continued presence of Gom A, the addition of sesamine failed to suppress  $I_{Na}$  further. Gom A also effectively suppressed the strength of persistent  $I_{Na}$  activated by long ramp voltage command, and further application of tefluthrin effectively attenuated Gom A-mediated inhibition of the current. The presence of Gom A mildly inhibited erg-mediated K<sup>+</sup> current, while a lack of change in the amplitude of hyperpolarization-activated cation current was observed in its presence. Under cell-attached current recordings, the exposure to Gom A resulted in the decreased firing of spontaneous action currents with a minimal change in AC amplitude. In pancreatic INS-1 cells, the presence of Gom A was also noticed to inhibit peak and end-pulse components of  $I_{Na}$  differentially with the IC<sub>50</sub> of 5.9 and 0.84 μM, respectively. Taken together, the emerging results presented herein provide the evidence that Gom A can differentially inhibit peak and sustained  $I_{Na}$  in endocrine cells (e.g., GH<sub>3</sub> and INS-1 cells).

**Keywords:** Gomisin A; voltage-gated Na<sup>+</sup> current; erg-mediated K<sup>+</sup> current; current kinetics; action current; excitable cell

## 1. Introduction

Gomisin A (Gom A, wuweizichu B, wǔwèizi chún yǐ), a dietary dibenzocyclooctadiene lignan compound isolated from the hexane of *Schisandra chinensis* fruit extract [1–6], has been increasingly demonstrated to have anti-inflammatory, anti-oxidative, antihypertensive, neuroprotective, and anti-proliferative properties [7–11]. For example, this compound was reported to induce protective effects either against hepatic and renal injury induced by CCl<sub>4</sub> exposure, or nitropropionic acid-induced striatal toxicity, through differential regulation of the MAPK signal transduction pathway [12,13]. It could inhibit COX-2, iNOS, IL-6, TNF- $\alpha$ , and NO through the downregulation of RIP2 and NF- $\kappa$ B activation in mouse macrophages [7,14,15]. Earlier reports have also shown that Gom A was able to exert anti-oxidative effects in osteoblast differentiation and in vascular endothelial cells [11,16], and to induce apoptotic changes in colon carcinoma HCT-116 cells [17]. Alternatively, the active components of *S. chinensis* were recently demonstrated to be detected after the intragastric administration of the lignans in rats [6].

Earlier studies have revealed that Gom A could suppress the contractility of penile corpus cavernosum smooth muscle and that this effect appears to be mediated from the NO-cyclic guanosine monophosphate pathway [18]. It has been also demonstrated that schisandrin, one of the major lignans isolated from *Schisandra chinensis*, could suppress spontaneous contraction in rat colon [19]. Additionally, the ability of crude *Schisandra chinensis* extracts to perturb the function of hypothalamic-pituitary-adrenal and gonadal axis in stressed rats has been previously reported [20,21]. The extracts of *S. chinensis* or *arisanensis* have been noticed to improve either amyloid- $\beta$ - and scopolamine-induced cognitive impairment or pancreatic  $\beta$ -cell function [9,10,22–25]. Of particular interest, an earlier study demonstrated the effectiveness of crude *S. chinensis* extract in decreasing prolactin production in pituitary GH<sub>3</sub> cells, suggesting that such an extract could be therapeutically beneficial for patients with hyperprolactinemia and prolactinoma [26].

Nine isoforms (Nav1.1–1.9) are present in mammalian excitable tissues, such as endocrine system [27,28]. Of notice, several inhibitors known to preferentially block the late component of voltage-gated Na<sup>+</sup> current ( $I_{Na}$ ), such as ranolazine and perampanel [29,30]. In particular, ranolazine has been demonstrated to exert the inhibitory action on the brain Nav channels for which mutations are associated with epilepsy; moreover, the isoforms of these channels studied are Nav1.1, Nav1.2, Nav1.3 and Nav1.6. Those are typically studied in heterologous expression in mammalian cells and in some cases with transgenic mice [31]. Effect of *S. chinensis* extracts (i.e., schizandrol A) on anti-epileptic activity has been reported [32,33]. However, how Gom A or other related compounds is capable of interacting with Nav channels to alter the strength and/or gating of  $I_{Na}$  in different types of electrically excitable cells largely remains elusive, although previous reports have demonstrated the ability of gomisin A or *S. chinensis* extracts to perturb the strength of transient receptor potential vanilloid type1 [15,34].

In light of the above-mentioned statements, the objective of this work was to investigate whether the presence of Gom A could exert any modifications on the amplitude or gating of  $I_{Na}$  identified from pituitary tumor (GH<sub>3</sub>) and pancreatic INS-1 cells. The present observations provide the evidence to show, first and foremost, that cell exposure to Gom can effectively and differentially decrease the magnitude of peak and end-pulse  $I_{Na}$ , in combination with an accentuation in the rate of current inactivation. Under cell-attached current recordings, its presence was also noticed to suppress the firing of spontaneous action currents (ACs) recorded from GH<sub>3</sub> cells. The reduction of AC firing caused by Gom A could be largely explained by its perturbations on the amplitude and/or gating of  $I_{Na}$  activated in response to rapid depolarization. Therefore, findings from this study provide novel insights into electrophysiological and pharmacological properties of Gom A or other related compounds (e.g., sesamine).

## 2. Results

### 2.1. Inhibitory Effect of Gom A on Voltage-Gated Na<sup>+</sup> Current ( $I_{Na}$ ) in Pituitary GH<sub>3</sub> Cells

In the first stage of experiments, we evaluated the possible modifications on  $I_{Na}$  caused by Gom A in these cells. We bathed cells in Ca<sup>2+</sup>-free Tyrode's solution, where Ca<sup>2+</sup> currents or Ca<sup>2+</sup>-activated K<sup>+</sup> currents are mostly diminished, and the recording electrode was backfilled with Cs<sup>+</sup>-containing solution. As the whole-cell current recordings became established (i.e., membrane patch under the electrode was abruptly broken by suction), the examined cells were clamped at the level of −80 mV, and an abrupt 50-msec membrane depolarization to −10 mV followed by return to −50 mV was thereafter applied (Figure 1). Under this experimental profile, an inward current activated in response to brief depolarizing step was evoked, and it was regarded as an  $I_{Na}$  [35]. After 1 min of continuous exposure of cells to Gom A, a concentration-dependent drop in the amplitude of both peak and end-pulse components of  $I_{Na}$  was noticed, concurrently with an evident increase in the inactivation and deactivation rate of the current (Figure 1A,B), despite a lack of change in the activation rate of the current was demonstrated in the presence of Gom A. For example, the addition of 3 μM Gom A resulted in a reduction of current amplitude at the start of depolarizing voltage command from  $447 \pm 28$  to  $318 \pm 21$  pA ( $n = 8, p < 0.05$ ). After the agent was washed out, the current amplitude returned to  $438 \pm 25$  pA ( $n = 7, p < 0.05$ ). Moreover, apart from the inhibition of current magnitude, the value of time constant in the slow component of current inactivation ( $\tau_{inact(S)}$ ) taken in response to brief depolarization, was concurrently diminished during the exposure to this agent (Figure 1A,B). For example, the addition of 3 μM Gom A to the bath resulted in a noticeable decrease in the  $\tau_{inact(S)}$  value to  $11.1 \pm 0.8$  msec ( $n = 8, p < 0.05$ ) from a control value of  $23.4 \pm 1.2$  msec ( $n = 8$ ). Meanwhile, in the presence of 3 μM Gom A, the time constant of deactivating  $I_{Na}$  obtained following return to the level of −50 mV was decreased from  $22.9 \pm 1.1$  to  $12.2 \pm 0.9$  msec ( $n = 8, p < 0.05$ ). However, the value for the time constant in neither current activation rate nor the fast component in the inactivation time constant of the current was modified in the presence of 3 μM Gom A. Alternatively, the value of  $dI/dt$  during rapid rising phase of  $I_{Na}$  remained unchanged in the presence of 3 μM Gom A ( $256 \pm 14$  pA/msec; control) versus  $257 \pm 16$  pA/msec (in the presence of Gom A),  $n = 8, (p > 0.05)$ , suggesting that the activation kinetics was not altered in its presence.

The depressant effect of Gom A with different concentrations on the peak or end-pulse component of  $I_{Na}$  activated by 50-msec short depolarization was thereafter evaluated. The concentration-dependent relationship of the inhibitory effect of this agent on  $I_{Na}$  amplitude (i.e., peak and end-pulse  $I_{Na}$ ) in GH<sub>3</sub> cells was derived and is hence illustrated in Figure 1C. According to the modified Hill equation stated under "Materials and Methods", the resultant concentration-dependent relationships were analyzed with least-squares approximation, the IC<sub>50</sub> value of Gom A which was needed for the inhibition of transient or late  $I_{Na}$  was then yielded to be 6.2 or 0.73 μM, respectively. The results enable us to suggest that the exposure to Gom A could differently and effectively decrease the amplitude of transient and late  $I_{Na}$ .

### 2.2. Evaluation of Time-Dependent Attenuation of $I_{Na}$ Inactivation Caused by the Presence of Gom A

It was noticeable that increasing Gom A not simply led to decreased amplitude in the peak  $I_{Na}$ , but it produced an evident elevation in the strength of current inactivation as well. On the basis of the first-order reaction scheme elaborated under "Materials and Methods", the relationship between  $1/\tau_{inact(S)}$  and the Gom A concentration was then approximated to be linear with a correlation coefficient of 0.97 (Figure 1D). As the values of both slope and y-intercept were evaluated, the resultant forward ( $k_{+1}^*$ ) or backward ( $k_{-1}$ ) rate constant was calculated to  $20.7 \text{ s}^{-1} \cdot \mu\text{M}^{-1}$  or  $34.0 \cdot \text{s}^{-1}$ , respectively. Owing to these rate constants, the apparent dissociation constant (i.e.,  $K_D = k_{-1}/k_{+1}^*$ ) required for the binding of Gom A to Na<sub>v</sub> channels was consequently yielded to be 1.64 μM. Of interest, this value is closely similar to the estimated IC<sub>50</sub> value for Gom A-perturbed inhibition of late  $I_{Na}$  determined from the concentration-response curve described above (Figure 1C).

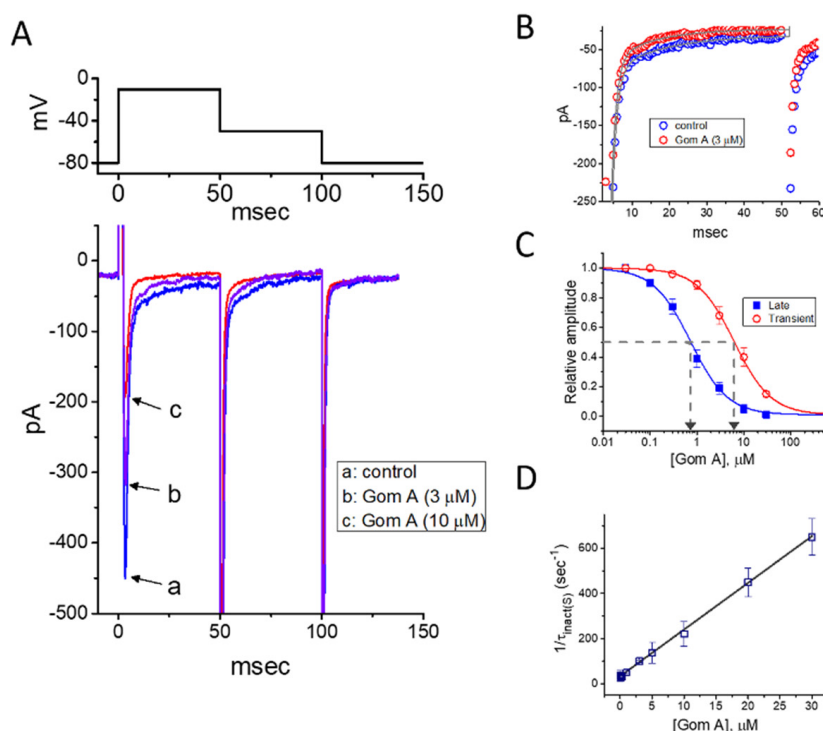


**Figure 1.** Inhibitory effect of Gom A on voltage-gated  $\text{Na}^+$  current ( $I_{\text{Na}}$ ) identified in pituitary tumor ( $\text{GH}_3$ ) cells. In these experiments, we bathed cells in  $\text{Ca}^{2+}$ -free Tyrode's solution which contained 10 mM tetraethylammonium chloride, and the pipette used was backfilled with  $\text{Cs}^+$ -containing solution. (A) Representative  $I_{\text{Na}}$  traces in response to membrane depolarization (indicated in the upper part). Current labeled a is control (i.e., Gom A was not present), and that labeled b or c was taken in the presence of 3 or 10  $\mu\text{M}$  Gom A. (B) Time course of  $I_{\text{Na}}$  inactivation trajectory activated by brief depolarization.  $\circ$ : control;  $\circ$ : in the presence of 3  $\mu\text{M}$  Gom A. The data point in each trace was reduced by a factor of 5 for better illustration. The continuous line indicated in the gray line was least-squares fit to two exponentials. The time constant in the slow component of current inactivation obtained without or with addition of 3  $\mu\text{M}$  Gom A was estimated to be 23.2 or 11.2 msec, respectively. (C) Concentration-dependent inhibitory effect of Gom A on the peak ( $\circ$ ) or end-pulse ( $\blacksquare$ ) component of  $I_{\text{Na}}$  activated by brief depolarizing pulse (mean  $\pm$  SEM;  $n = 9$ ). Current amplitudes at different concentrations of Gom A were taken at the beginning of the depolarizing pulse from  $-80$  to  $-10$  mV. The  $\text{IC}_{50}$  value required for Gom A-mediated inhibition of peak or end-pulse  $I_{\text{Na}}$  present in these cells (as indicated in arrow of the dashed vertical line) was calculated to be 6.2 or 0.73  $\mu\text{M}$ , respectively. (D) The relation of the reciprocal of  $\tau_{\text{inact(s)}}$  (i.e., slow component of current inactivation) versus the Gom A concentration (mean  $\pm$  SEM;  $n = 8$ ). The value of current inactivation was measured as the examined cell was rapidly depolarizing from  $-80$  to  $-10$  mV with a duration of 50 msec. According to minimal reaction scheme stated under "Materials and Methods", forward ( $k_{+1}^*$ ) or backward ( $k_{-1}$ ) rate constants, determined by the slope or the  $y$ -axis intercept of the interpolated line, was yielded to be  $20.7 \text{ s}^{-1} \cdot \mu\text{M}^{-1}$  or  $34.0 \text{ s}^{-1}$ , respectively.

### 2.3. Mean I-V Relationship and the Steady-State Inactivation Curve of Peak $I_{\text{Na}}$ Obtained in the Absence or Presence of Gom A

As demonstrated in Figure 2A, the effects of Gom A on peak  $I_{\text{Na}}$  were further examined at different membrane potentials, and an  $I$ - $V$  relationship of the current was established. The observed overall  $I$ - $V$  relationship of peak  $I_{\text{Na}}$  remained unchanged in the presence of 3  $\mu\text{M}$  Gom A. To characterize the inhibitory effect of Gom A on  $I_{\text{Na}}$ , we continued to explore whether there were any adjustments in the steady-state inactivation curve of peak  $I_{\text{Na}}$  during the exposure to this compound. The relationship of conductance versus membrane potential for peak  $I_{\text{Na}}$  taken with or without addition of 3  $\mu\text{M}$  GomA is illustrated in Figure 2B. Figure 2C depicts the steady-state inactivation curve taken without

or with addition of 3  $\mu\text{M}$  Gom A. The data with respect to the relationship of conditioning potential versus normalized amplitude of peak  $I_{\text{Na}}$  were established and then goodness-of-fit with a Boltzmann function described under “Materials and Methods”. The resultant value for half-maximal inactivation ( $V_{1/2}$ ) or the apparent gating charge ( $q$ ) in the control (i.e., Gom A was not present) was  $-21.2 \pm 1.0$  mV or  $4.3 \pm 0.7$  e ( $n = 7$ ), respectively, whereas, during the exposure to 3  $\mu\text{M}$  Gom A, the value of  $V_{1/2}$  or  $q$  was  $-32.2 \pm 1.1$  mV or  $4.4 \pm 0.7$  e ( $n = 7$ ), respectively. These data therefore enable us to reflect that the steady-state  $I_{\text{Na}}$  inactivation curve in the presence of Gom A was shifted in a leftward direction, with no evident adjustment in the gating charge of the current, and that this agent exerts depressant action on peak  $I_{\text{Na}}$  in a voltage-dependent fashion in these cells.

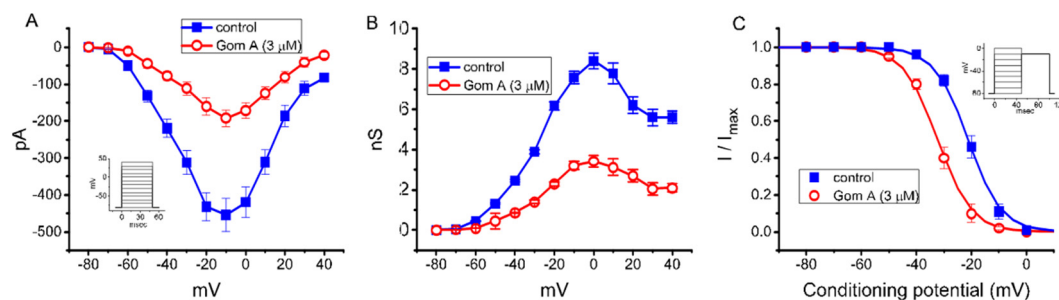


**Figure 2.** Effect of Gom A on mean current-voltage ( $I$ - $V$ ) relation, conductance versus voltage relation, and the steady-state inactivation curve of  $I_{\text{Na}}$  measured from  $\text{GH}_3$  cells. The experiments were conducted in cells bathed in  $\text{Ca}^{2+}$ -free Tyrode’s solution and we backfilled the solution by using  $\text{Cs}^+$ -containing solution. (A) Mean  $I$ - $V$  relation of peak  $I_{\text{Na}}$  in the absence (■) or presence (○) of 3  $\mu\text{M}$  Gom A (mean  $\pm$  SEM;  $n = 8$ ). Current amplitude was taken at the beginning of depolarizing voltage command. Of notice, the peak amplitude of  $I_{\text{Na}}$  was decreased after the addition of Gom A, with no change the overall  $I$ - $V$  relation of the current. (B) Mean conductance versus voltage relation of peak  $I_{\text{Na}}$  in the control (■) or during the exposure (○) to 3  $\mu\text{M}$  Gom A (mean  $\pm$  SEM;  $n = 8$ ). (C) Steady-state inactivation curve of  $I_{\text{Na}}$  obtained in the control (■) or during the exposure to 3  $\mu\text{M}$  Gom A (mean  $\pm$  SEM;  $n = 8$ ). The modified Boltzmann equation detailed under “Materials and Methods” was used to fit the experimental data with the goodness-of-fit test. Of notice, the presence of Gom A (3  $\mu\text{M}$ ) causes a leftward shift in the inactivation curve of the current by about 11 mV; however, no change in the gating charge of the current was demonstrated in its presence. Inset in (A,C) indicates the voltage-clamp protocol applied.

#### 2.4. Comparison of Effects of Morin, Hesperidin, Gom A, Sesamine, Gom A Plus Sesamine on Peak $I_{\text{Na}}$ Identified in $\text{GH}_3$ Cells

We also further evaluated and compared effects of different compounds (e.g., morin, hesperidin and sesamin) which could be contained in the extracts of *S. chinensis* (Figure 3) [35,36]. The addition of neither morin nor hesperidin was noticed to perturb the amplitude of peak  $I_{\text{Na}}$  activated by rapid membrane depolarization. However, as reported recently [35], when  $\text{GH}_3$ -cells were exposed to sesamine (3  $\mu\text{M}$ ), the peak amplitude of the current was significantly decreased. Morin and hesperidin contained in *S. chinensis* extracts are the phenolic compounds (i.e., flavonoid). Moreover, in the continued presence of Gom A (3  $\mu\text{M}$ ), subsequent application of sesamine (3  $\mu\text{M}$ ) failed to decrease the peak amplitude of  $I_{\text{Na}}$  further. It is therefore plausible to anticipate that Gom A and sesamine interact with similar motifs to perturb the strength and/or the gating of  $I_{\text{Na}}$  in these cells.



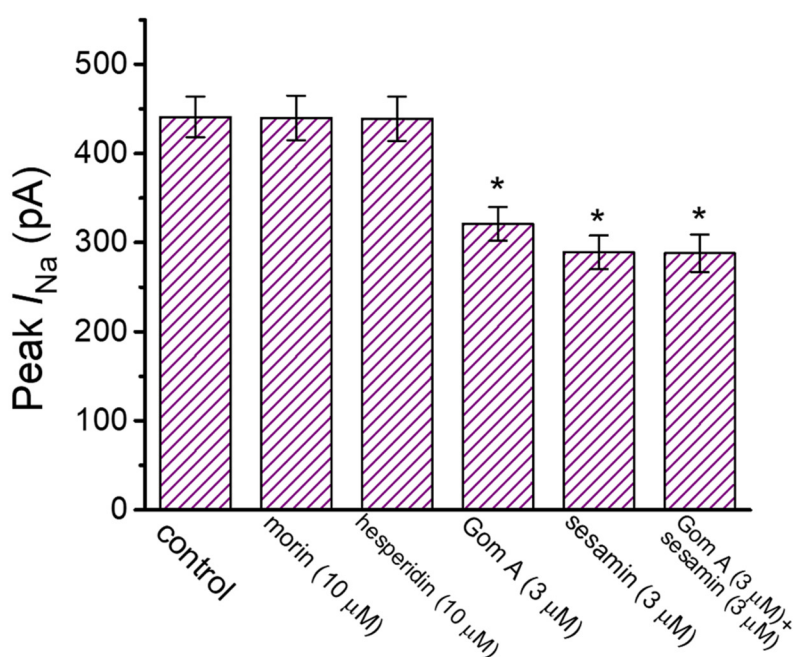


**Figure 3.** Comparison in effects of morin, hesperidin, Gom A, sesamine, Gom A plus sesamine on the amplitude of peak  $I_{Na}$  measured from GH<sub>3</sub> cells (mean  $\pm$  SEM;  $n = 7$ –8). The experiments were undertaken in cells bathed in Ca<sup>2+</sup>-free Tyrode's solution and we filled up the electrode with Cs<sup>+</sup>-containing solution. In an effort to activate  $I_{Na}$  in these cells, a 50-msec square voltage-clamp pulse to  $-10$  mV from the holding potential of  $-80$  mV was delivered to the examined cell, and current amplitude was measured at the start of depolarizing pulse. \* Significantly different from control ( $p < 0.05$ ).

### 2.5. The Amplitude of Persistent Na<sup>+</sup> Current ( $I_{Na(P)}$ ) Decreased by Gom A

We continued to explore whether the presence of Gom A could be able to perturb the strength of  $I_{Na(P)}$  measured from GH<sub>3</sub> cells. As the whole-cell current recordings were established, we held the cell in voltage clamp at  $-50$  mV and a 1-s ramp pulse from  $-100$  to  $+50$  mV was applied to evoke  $I_{Na(P)}$  [37]. Of notice, when the cells were exposed to  $1 \mu$ M Gom A, the amplitude of  $I_{Na(P)}$  activated under such slow ramp command was diminished (Figure 4A,B), as demonstrated by a conceivable reduction of current amplitude (i.e., measured at the level of  $-10$  mV) from  $145 \pm 22$  to  $55 \pm 7$  pA ( $n = 7$ ,  $p < 0.05$ ). After washout of the agent,  $I_{Na(P)}$  amplitude at the same level of membrane potential was returned to  $141 \pm 19$  pA ( $n = 7$ ,  $p < 0.05$ ). Moreover, during the continued exposure to  $1 \mu$ M Gom A, subsequent application of tefluthrin ( $10 \mu$ M) was able to counteract Gom A-attenuated amplitude of  $I_{Na(P)}$  effectively in GH<sub>3</sub> cells, as evidenced by the increase of  $I_{Na(P)}$  amplitude to  $121 \pm 19$  ( $n = 7$ ,  $p < 0.05$ ). Tefluthrin, a type-I pyrethroid insecticide, was previously demonstrated to augment the strength and inactivation time constant of  $I_{Na}$  [37–39]. It is conceivable, therefore, that Gom A effectively suppresses the amplitude of  $I_{Na(P)}$  in response to the long ramp pulse. Moreover, as cells were continually exposed to Gom A ( $1 \mu$ M), subsequent addition tetrodotoxin ( $1 \mu$ M) effectively decreased  $I_{Na(P)}$  elicited in response to such ramp pulse to  $5 \pm 1$  pA ( $n = 7$ ,  $p < 0.05$ ). Of notice, the presence of Gom A ( $1 \mu$ M) could decrease  $I_{Na(P)}$  by 62%, while it diminished the peak or end-pulse component of  $I_{Na}$  by 11% or 61%, respectively.

### 2.6. Effect of Gom A and Gom A Plus Ranolazine on erg-mediated K<sup>+</sup> Current ( $I_{K(erg)}$ )

We further extended to determine whether Gom A might perturb voltage-gated K<sup>+</sup> current (e.g.,  $I_{K(erg)}$ ) in GH<sub>3</sub> cells. In attempts to amplify the magnitude of  $I_{K(erg)}$  [29,40], the experiments were conducted in cells bathed in high-K<sup>+</sup>, Ca<sup>2+</sup>-free solution, while the recording pipette was filled with K<sup>+</sup>-containing solution. The compositions of these solutions were detailed under "Materials and

Methods". In these experiments, to evoke  $I_{K(\text{erg})}$ , the examined cell was 1-sec hyperpolarized from  $-10$  to  $-100$  mV. As cells were exposed to Gom A at a concentration of  $3 \mu\text{M}$ , no significant change in  $I_{K(\text{erg})}$  amplitude was demonstrated ( $815 \pm 61$  pA [control] versus  $812 \pm 64$  pA [in the presence of  $3 \mu\text{M}$  Gom A],  $n = 7$ ,  $p > 0.05$ ). However, as depicted in Figure 5A, the addition of  $10 \mu\text{M}$  Gom A was noticed to decrease the amplitude of deactivating  $I_{K(\text{erg})}$  significantly from  $812 \pm 59$  to  $687 \pm 52$  pA ( $n = 8$ ,  $p < 0.05$ ). After the agent was washed out, current amplitude became returned to  $807 \pm 58$  pA ( $n = 7$ ,  $p < 0.05$ ). Moreover, as cells were continually exposed to  $10 \mu\text{M}$  Gom A, further application of ranolazine ( $10 \mu\text{M}$ ) resulted in an additional reduction of current amplitude, as demonstrated by the decrease of  $I_{K(\text{erg})}$  amplitude to  $334 \pm 32$  pA ( $n = 8$ ,  $p < 0.05$ ). Apart from being a blocker of late  $I_{\text{Na}}$ , ranolazine has been previously reported to modify the amplitude and gating of  $I_{K(\text{erg})}$  [29,33]. Alternatively, as cells were continually exposed to  $10 \mu\text{M}$  Gom A, further addition of E-4031 ( $10 \mu\text{M}$ ), a blocker of  $I_{K(\text{erg})}$  fully abolished  $I_{K(\text{erg})}$  amplitude. The mean  $I$ - $V$  relationships of  $I_{K(\text{erg})}$  obtained in the control and in the presence of  $10 \mu\text{M}$  Gom A or  $10 \mu\text{M}$  Gom A plus  $10 \mu\text{M}$  ranolazine were constructed and are hence illustrated in Figure 5B. Under our voltage-clamp conditions, the experimental observations led us to suggest that, distinguishable from  $I_{\text{Na}}$ , the  $I_{K(\text{erg})}$  inherently in GH<sub>3</sub> cells is to some extent relatively resistant to being blocked by Gom A.

### 2.7. Failure of Gom A to Alter Hyperpolarization-Activated Cation Current ( $I_h$ ) in GH<sub>3</sub> Cells

In a separate set of experiments, we continued to test whether this agent produced any effect on the amplitude and/or gating of  $I_h$  inherently in these cells [35,41]. To measure  $I_h$ , cells were bathed in  $\text{Ca}^{2+}$ -free Tyrode's solution and we filled the electrode by using  $\text{K}^+$ -containing solution. As shown in Figure 6A, when the 2-s hyperpolarizing pulse from  $-40$  to  $-110$  mV was applied to the cell, the  $I_h$  with the slowly activating time course was readily evoked [35,41]. However, as cells were exposed to  $10 \mu\text{M}$  Gom A, neither the amplitude nor gating of  $I_h$  were perturbed ( $69 \pm 7$  pA [in the control] versus  $69 \pm 8$  pA [in the presence of Gom A],  $n = 8$ ,  $p > 0.05$ ). Moreover, in the continued presence of  $10 \mu\text{M}$  Gom A, subsequent addition of  $10 \mu\text{M}$  croton-03 was able to decrease  $I_h$  amplitude effectively, as demonstrated by a significant reduction of current amplitude to  $25 \pm 6$  pA ( $n = 8$ ,  $p < 0.05$ ). Similarly, as cells were continually exposed to  $10 \text{mM}$  Gom A, further application of  $10 \mu\text{M}$  ivabradine, a blocker of  $I_h$ , fully abolished  $I_h$  amplitude. Figure 6B illustrates the mean  $I$ - $V$  relationships of  $I_h$  (measured at the end of each hyperpolarizing step) taken in the control and during the exposure to  $10 \mu\text{M}$  Gom A or  $10 \mu\text{M}$  Gom A plus  $10 \mu\text{M}$  croton-03. As such, consistent with previous reports [42], the present observations showed that croton-03 was effective at inhibiting  $I_h$ . However, lack of change in  $I_h$  amplitude or gating was demonstrated in the presence of Gom A alone. Unlike  $I_{\text{Na}}$ , the hyperpolarization-activated  $I_h$  identified in these cells is subject to be resistant to the modification by Gom A.

### 2.8. Inhibitory Effect of Gom A on Spontaneous Action Currents (ACs) Identified in GH<sub>3</sub> Cells

We then continued to examine whether Gom A had any effects on AC firing in these cells. In these cell-attached current recordings, we immersed cells in normal Tyrode's solution containing  $1.8 \text{mM}$   $\text{CaCl}_2$ , and we then voltage-clamped the examined cell at the resting potential. As demonstrated in Figure 7, the addition of different concentrations ( $1$  and  $3 \mu\text{M}$ ) of Gom A diminished the AC frequency significantly. However, no change in AC amplitude was noticed in its presence. For example, as cell cells were exposed to Gom A ( $3 \mu\text{M}$ ), the firing frequency of ACs detected in GH<sub>3</sub> cells was decreased to  $0.6 \pm 0.1$  Hz ( $n = 7$ ,  $p < 0.05$ ) from a control value of  $1.6 \pm 0.2$  Hz ( $n = 7$ ). After this agent was washed out, the firing frequency was returned to  $1.5 \pm 0.2$  Hz ( $n = 7$ ,  $p < 0.05$ ). It is conceivable, therefore, that the Gom A-perturbed reduction of AC firing in these cells is closely linked to its inhibition of  $I_{\text{Na}}$  described above.

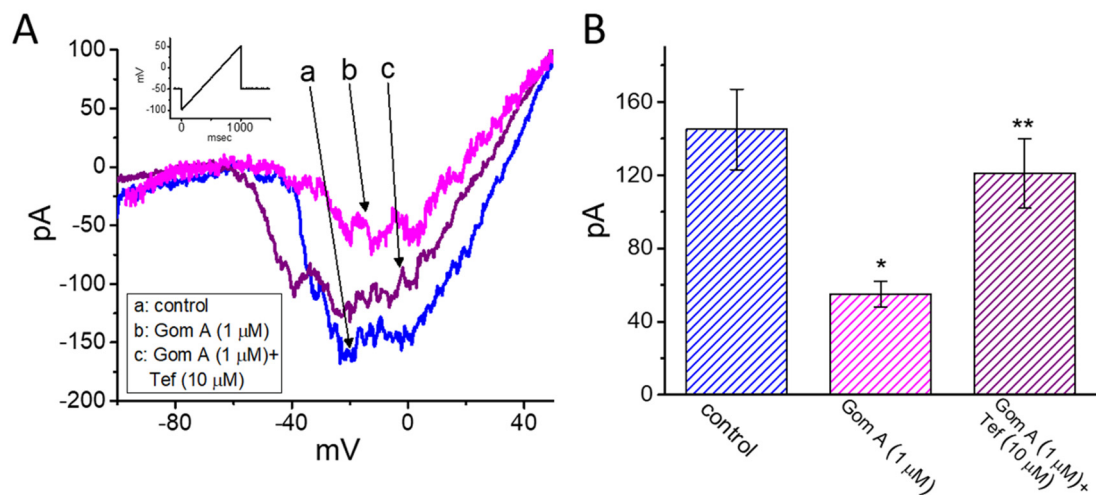


**Figure 4.** Effects of Gom A and Gom A plus tefluthrin on the persistent component of  $I_{Na}$  ( $I_{Na(P)}$ ) in GH<sub>3</sub> cells. The whole-cell current recordings were conducted in cells which was activated by a sec long ramp pulse from  $-100$  to  $+50$  mV. (A) Representative current traces obtained in the control (i.e., Gom A was not present, a) and during the exposure to  $1 \mu\text{M}$  Gom A (b) or  $1 \mu\text{M}$  Gom A plus  $10 \mu\text{M}$  tefluthrin (Tef) (b). Inset indicates the voltage protocol applied. (B) Summary bar graph showing effects of Gom A and Gom A plus tefluthrin on the amplitude of  $I_{Na(P)}$  (i.e., tetrodotoxin-sensitive current) (mean  $\pm$  SEM;  $n = 7$ ). Current amplitude was measured at the level of  $-10$  mV when the examined cell was ramp-pulsed from  $-100$  to  $+50$  mV with a duration of 1 sec. \* indicates significantly from control ( $p < 0.05$ ) and \*\* significantly from  $1 \mu\text{M}$  Gom A alone group ( $p < 0.05$ ).

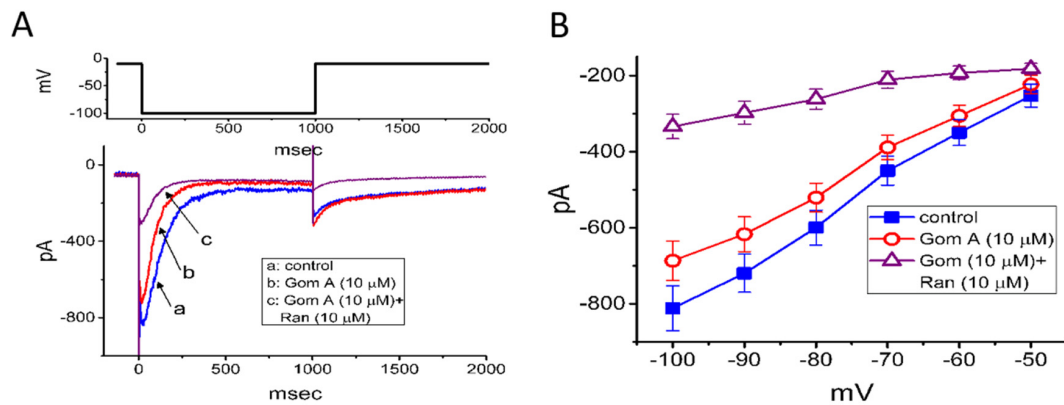


**Figure 5.** Mild inhibition of erg-mediated  $K^+$  current caused by Gom A in GH<sub>3</sub> cells. In this set of experiments, cells were bathed in high- $K^+$ ,  $Ca^{2+}$ -free solution containing  $1 \mu\text{M}$  tetrodotoxin and, for current recordings, we backfilled the pipette by using  $K^+$ -containing solution. (A) Representative  $I_{K(erg)}$  traces obtained in the absence (a) and presence of  $10 \mu\text{M}$  Gom A (b) or  $10 \mu\text{M}$  Gom A plus  $10 \mu\text{M}$  ranolazine (Ran, c). The upper part shows the voltage protocol delivered. (B) Mean I-V relationship of  $I_{K(erg)}$  taken in the control (■) and during cell exposure to  $10 \mu\text{M}$  Gom A (○) or  $10 \mu\text{M}$  Gom A plus  $10 \mu\text{M}$  ranolazine (mean  $\pm$  SEM;  $n = 7$ ). Current amplitude was taken at the beginning of each hyperpolarizing step.



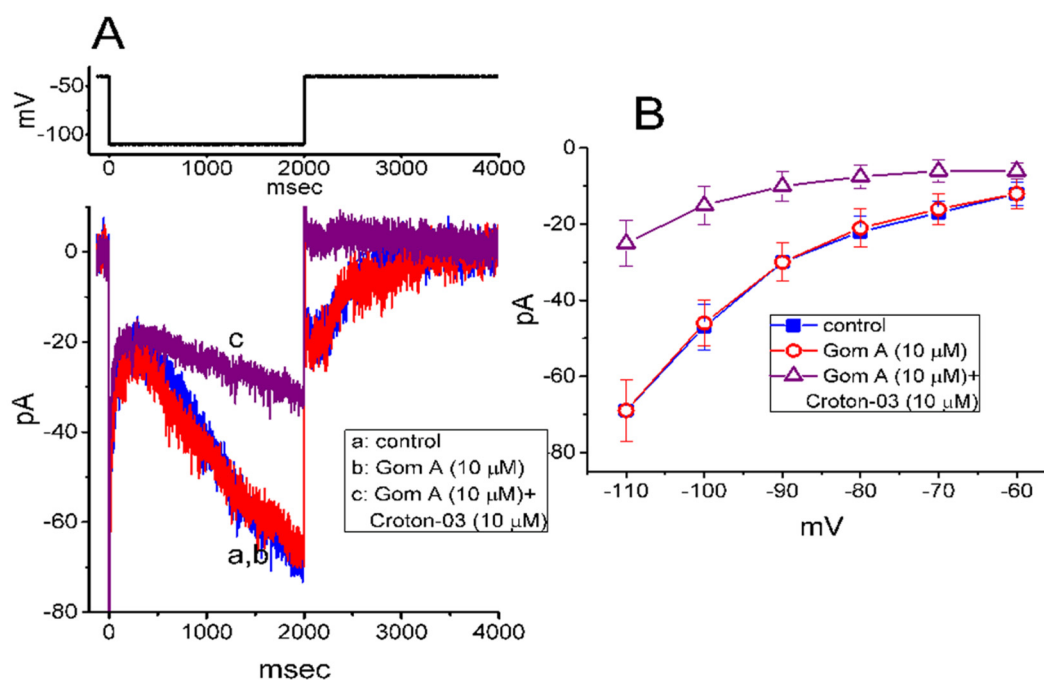


**Figure 6.** Inability of Gom A to inhibit hyperpolarization-activated cation current ( $I_h$ ) in GH3 cells. In this set of whole-cell experiments, we bathed cells in  $Ca^{2+}$ -free Tyrode's solution containing 1  $\mu M$  tetrodotoxin and we filled the backfilling solution with  $K^+$ -containing solution. (A) Representative  $I_h$  traces taken in the absence (a) and presence of 10  $\mu M$  Gom A (b) or 10  $\mu M$  Gom A plus 10  $\mu M$  croton-03 (c). The voltage protocol used is illustrated in the upper part. (B) Mean I-V relationship of  $I_h$  (i.e., ivabradine-sensitive current) collected in the control (■) and during cell exposure to 10  $\mu M$  Gom A (○) or 10  $\mu M$  Gom A plus 10  $\mu M$  croton-03 (mean  $\pm$  SEM;  $n = 8$ ). The cell examined was held at  $-10$  mV and a series of hyperpolarizing commands ranging between  $-110$  and  $-60$  mV with a duration of 2 sec were delivered. Current amplitude was taken at the end of each hyperpolarizing step applied.

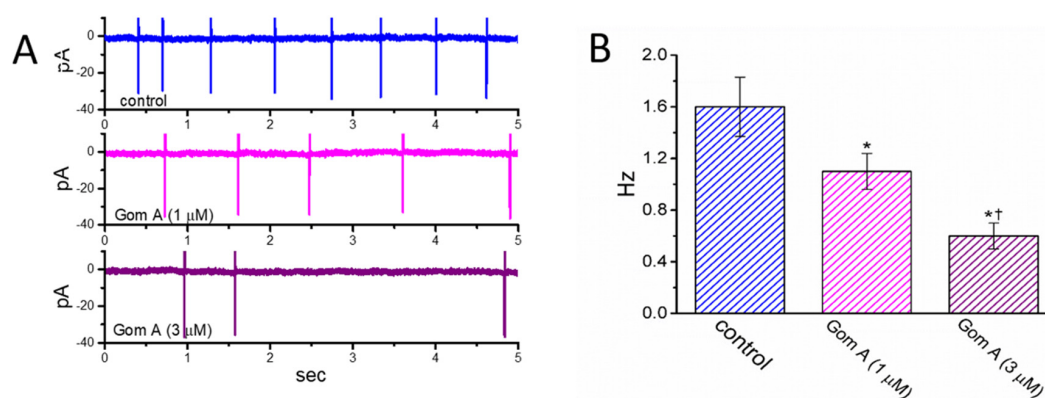


**Figure 7.** Inhibitory effect of Gom A on the firing of action currents (ACs) recorded from voltage-clamped GH3 cells. In this set of cell-attached current recordings, we bathed cells in normal Tyrode's solution which contained 1.8 mM  $CaCl_2$ , the electrode was filled with  $K^+$ -containing solution, and the potential was maintained at the resting of the cell ( $\sim -70$  mV). (A) Representative AC traces obtained in the control (upper) and during cell exposure to 1  $\mu M$  Gom A (middle) or 3  $\mu M$  Gom A (lower). Of notice, the inward deflection in each traces indicates the occurrence of AC. (B) Summary bar graph showing inhibitory effect of Gom A (1 and 3  $\mu M$ ) on the firing frequency of spontaneous ACs identified from these cells (mean  $\pm$  SEM;  $n = 8$ ). \* indicates significantly different from control ( $p < 0.05$ ) and  $^\dagger$  significantly different from Gom A (1  $\mu M$ ) alone group ( $p < 0.05$ ).

### 2.9. Effect of Gom A on $I_{Na}$ in INS-1 Cells

The extracts of *S. chinensis* or *arisanensis* have been previously demonstrated to modify pancreatic  $\beta$ -cell function [23,25,43]. Ranolazine, known to be an inhibitor of late  $I_{Na}$ , has been previously noticed to influence glycemic control [44]. Therefore, in a final set of experiments, effects of Gom A on another type of electrically excitable endocrine cells (i.e., INS-1 cells) were further evaluated. INS-1 cells were bathed  $Ca^{2+}$ -free Tyrode's solution and we filled up the recording pipette by using  $Cs^{+}$ -containing solution. As depicted in Figure 8, as INS-1 cells were exposed to different concentrations (0.03–30  $\mu M$ ) of Gom A, the amplitude of  $I_{Na}$  was progressively decreased. The effective  $IC_{50}$  value of Gom A-perturbed inhibition of peak or end-pulse component of  $I_{Na}$  was estimated to be 5.9 or 0.84  $\mu M$ , respectively. Findings from these experimental data are in keeping with those elaborated above in GH<sub>3</sub> cells.

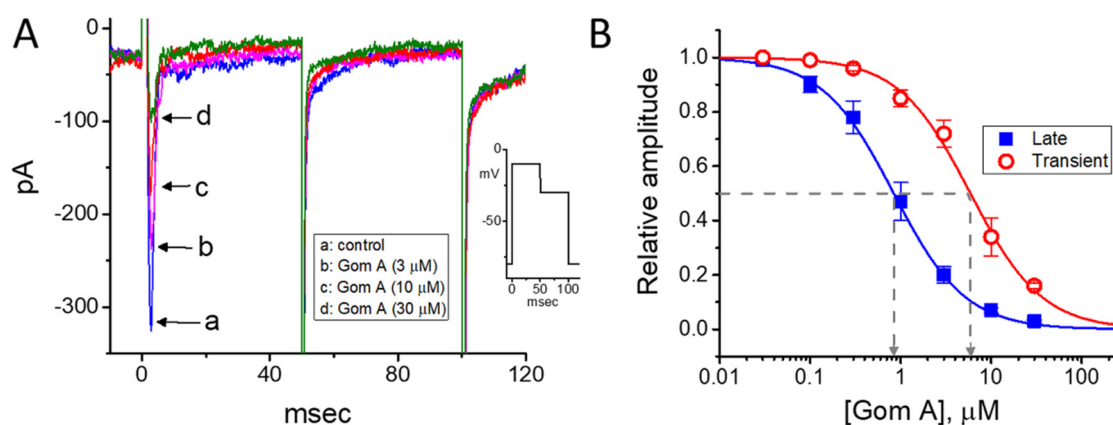


**Figure 8.** Inhibitory effect of Gom A on  $I_{Na}$  measured from pancreatic INS-1 cells. Cells were bathed in  $Ca^{2+}$ -free Tyrode's solution containing  $CdCl_2$  (0.5 mM). (A) Representative  $I_{Na}$  traces obtained in the absence (a) and presence of 3  $\mu M$  Gom A (b), 10  $\mu M$  Gom A (c), or 30  $\mu M$  Gom A (d). As indicated in inset of (A), in these experiments, the hold potential was set at  $-80$  and the 50-msec depolarizing pulse to  $-10$  mV followed by a return to the level of  $-30$  mV with a duration of 50 msec. (B) Concentration-dependent inhibition of peak (■) or end-pulse (○) component of  $I_{Na}$  by Gom A. Current amplitude during the exposure to different concentrations of Gom A was taken at the beginning of depolarizing pulse from  $-80$  to  $-10$  mV. By use of least-squares non-linear regression approximation, the  $IC_{50}$  value required for Gom A-mediated inhibition of transient or late  $I_{Na}$  observed in these cells (as indicated in arrow of the dashed vertical line) was yielded to be 5.9 or 0.84  $\mu M$ , respectively.

### 3. Discussion

The present results demonstrated that the presence of Gom A was able to produce an inhibitory action on  $I_{Na}$  in GH<sub>3</sub> cells in a concentration-, a time- and state-dependent manner. Cell exposure to Gom A was also noticed to accentuate the rate of  $I_{Na}$  inactivation, particularly at the slow component of current inactivation. The inhibitory action on  $I_{Na}$  tended to be rapidly developing and readily washed out, and it would concurrently correlate in time with a significant raise in the inactivation rate of the current activated by short depolarizing pulse, while the activation kinetics of  $I_{Na}$  remained unchanged in the presence of Gom A. The observed effect of Gom A on the strength and gating  $I_{Na}$  primarily ascribed from this molecule acting largely on the  $Na_V$  channel itself or its accessory subunits.

In pituitary GH<sub>3</sub> cells, Gom A, known to be a lignan isolated from *S. chinensis*, differentially and effectively inhibited the transient or late components of  $I_{Na}$  with effective  $IC_{50}$  value of 6.2 or 0.73  $\mu M$ , respectively. According to minimal binding scheme, the approximated  $K_D$  value for Gom A-perturbed raise in current inactivation was also calculated to be 1.64  $\mu M$ , a value that tends to be similar to that needed to lessen the magnitude of late component of  $I_{Na}$ . It is therefore possible that the Gom A molecule preferentially binds to and interacts with the open state or conformation of the  $Na_V$  channel, hence producing a conceivable reduction in both amplitude and inactivation time constant

of  $I_{Na}$ . The presence of this agent was also noticed to inhibit the amplitude of  $I_{Na(P)}$  activated by a long ramp pulse, and its inhibition of  $I_{Na(P)}$  was able to be attenuated by subsequent addition of tefluthrin, an activator of  $I_{Na}$  [37,39]. Therefore, the Gom A-mediated reduction in  $I_{Na(P)}$  could also be explained by the accelerated deactivation of  $Na_V$  channel, and the possibility that Gom A might bind preferentially to the inactivated state of the channel could not be excluded. Under our cell-attached current recordings, the observed reduction of AC firing caused by Gom A could be largely explained by its effectiveness in the inhibition of peak and end-pulse  $I_{Na}$  measured from GH<sub>3</sub> cells. However, further studies are still needed to evaluate the extent to which this compound has therapeutic relevance in the treatments of patients with hyperprolactemia or prolactinoma as demonstrated previously [26].

In our study, the addition of Gom A was not only able to decrease the maximal conductance of peak  $I_{Na}$  but caused a negative (leftward) shift in the steady-state inactivation curve of the current as well. The lack of any change in the gating charge of the inactivation curve during the exposure to this agent thus enables us to indicate that the interaction with the  $Na_V$  channel is not mediated by a direct effect on the voltage sensor per se and that its binding site is likely to lie outside of the transmembrane field of the channel. An important consequence of a leftward shift of the inactivation curve is the decreased membrane excitability at voltages near the resting potential, accompanied by lessened AC firing identified in GH<sub>3</sub> cells. Under this scenario, the sensitivity of Gom A in non-voltage-clamped neurons or endocrine cells would rely on various confounding factors that include the preexisting level of resting potential, the firing of spontaneous action potentials, and the concentration of Gom A applied.

Gom A was recently demonstrated to penetrate into brain tissue [6,45]. Moreover, the plasma concentration of Gom A measured after oral administration in rats was previously reported to reach around 17  $\mu$ M [46], a value that is noticeably higher than the IC<sub>50</sub> values for Gom A-mediated inhibition of both peak and end-pulse  $I_{Na}$  measured from GH<sub>3</sub> and INS-1 cells. Therefore, our experimental observations demonstrating the effectiveness of Gom A in modifying membrane ionic currents, which tend to be upstream of its anti-oxidative properties [7,11,14,15], would enable us to indicate that these actions could be one of the underlying ionic mechanisms responsible for its perturbations on membrane excitability in different types of electrically excitable cells (e.g., GH<sub>3</sub> and INS-1 cells).

In this study, the presence of neither morin nor hesperidin was found to have any changes on the peak  $I_{Na}$ , while sesamine, another lignan, effectively inhibited the strength of the current as disclosed previously [35]. Therefore, Gom A or sesamine, which could be the important constituents contained in *S. chinensis* extracts, was capable of participating in the depressant action on  $I_{Na}$ . However, the inability of subsequent application of sesamine to perturb Gom-A-mediated inhibition of peak  $I_{Na}$  further, led us to imply that these two compounds tend to bind to similar motifs to interact with the  $Na_V$  channel. Of notice, according to modeled  $Na_V$  (i.e., SCN8A-encoded or  $Na_V1.6$ ) channels originally developed from a Markovian process (i.e., modified Pan-Cummins model) [47], it seems plausible to anticipate, therefore, that the "Oon", which represents the on rate of normal inactivation from the open state of the channel, could be a noticeable variable with which Gom A and/or sesamine could interact [35].

Previous work has also unraveled the ability of ranolazine, an inhibitor of late  $I_{Na}$ , to suppress  $I_{K(erg)}$  amplitude effectively [29,48,49]. However, in this study, Gom A at a concentration of 10  $\mu$ M only mildly inhibited the amplitude of deactivating  $I_{K(erg)}$  responding to long-lasting hyperpolarization. Further application of ranolazine (10  $\mu$ M) or E-4031 (10  $\mu$ M), still in the continued presence of Gom A, was effective at decreasing  $I_{K(erg)}$  further. Additionally, there appears to be void of modifications in the strength and gating of  $I_h$  in the presence of Gom A. Therefore, by comparison with the ranolazine action, the inhibitory effect of Gom A on  $I_{Na}$  identified from GH<sub>3</sub> or INS-1 cells could be to some extent more specific.

The binding scheme presented in this study enables us to suggest the recovery of  $Na_V$  channels from the open state. However, of notice,  $Na_V$ -channel isoforms might differ very specifically for this transition. Most isoforms are able to recover from the inactivated to the closed (or resting) state, although open-state recovery observed in a few isoforms (e.g., SCN8A-encoded or  $Na_V1.6$  current).

The  $I_{NaV}$  isoforms in these cell lines (i.e., GH<sub>3</sub> and INS-1 cells) have not been identified and this minimal scheme could therefore make an assumption that may not be valid. Additionally, the  $I_{Na(P)}$  itself is not an indicator of open-state recovery. Taken together, the scheme demonstrated herein does not account for the presence of the closed-state inactivation. As such, it would be interesting to evaluate whether the  $I_{NaV}$  isoforms in the cells studied are able to transit to the inactivated state without opening activated in response to weak depolarization. In muscle and neuronal  $I_{NaV}$  channels this state transition is the dominant parameter for steady-state inactivation and is a target of channelopathy-mediated gating defects [50]. It also remains to be further studied with respect to the extent what Gom A or other structurally similar compounds could interact with different isoforms of  $I_{NaV}$  channels to modify the strength and kinetics of  $I_{Na}$ .

Our study was also extended to demonstrate that, in INS-1 cells, similar to the ranolazine on  $I_{Na}$  [49], the presence of Gom A was efficacious at inhibiting  $I_{Na}$  activated by rapid depolarization. The  $IC_{50}$  value for its inhibition of peak or end-pulse  $I_{Na}$  in these cells was yielded to be 5.9 or 0.84  $\mu$ M, respectively. The experimental observations, therefore, enable us to anticipate that Gom A-mediated inhibition of  $I_{Na}$  observed in pancreatic  $\beta$ -cells could be closely linked to its perturbations on electrical behavior or other functional activities in various types of electrically excitable cells [18,19,26]. The inhibitory actions presented herein allowed us to provide important insights into the underlying ionic mechanism for Gom A actions [4,8,26].

## 4. Materials and Methods

### 4.1. Chemicals, Drugs and Solutions Used in This Study

Gomisin A (Gom A, wǔwèizi chún yǐ, CFN98990, besigomisin, schisandrin B, schisandrol B, schisantherinol B, schizandrol B, TJN-101; wuwizi alcohol B, wuweizichun B, (6S,7S,13aR)-5,6,7,8-tetrahydro-1,2,3,13-tetramethoxy-6,7-dimethyl-benzo[3,4]cycloocta[1,2-f][1,3]benzodioxol-6-ol, C<sub>23</sub>H<sub>28</sub>O<sub>7</sub>, PubChem CID: CID-3001662), heresperin, and morin were acquired from ChemFaces (Rainbow Biotechnology, Taipei, Taiwan), and E-4031, ivabradine,  $\beta$ -mercaptoethanol, sodium pyruvate, tetrodotoxin, and trypan blue were from Sigma-Aldrich (Merck, Taipei, Taiwan), while ranolazine was from Tocris (Union Biomed, Taipei, Taiwan). Croton-03 or sesamine was kindly provided by Dr. Ping-Chung Kuo (School of Pharmacy, National Cheng Kung University Medical College, Tainan, Taiwan). Unless stated otherwise, culture media (e.g., Ham's F12 and RPMI-1460 media), fetal bovine or calf serum, horse serum, L-glutamine, and trypsin/EDTA were acquired from HyClone™ (Thermo Fisher, Level Biotech, Tainan, Taiwan), while other chemicals or reagents, such as CsOH, CsCl<sub>2</sub>, CdCl<sub>2</sub>, EGTA and HEPES, were of analytical grade.

The HEPES-buffered normal Tyrode's solution used in this study had a composition, which comprised (in mM): NaCl 136.5, KCl 5.4, CaCl<sub>2</sub> 1.8, MgCl<sub>2</sub> 0.53, glucose 5.5, and HEPES 5.5 adjusted to pH 7.4 with NaOH. For the measurement of  $I_{Na}$  or  $I_h$ , we bathed cells in Ca<sup>2+</sup>-free Tyrode's solution in order to minimize the contamination of Ca<sup>2+</sup>-activated K<sup>+</sup> currents and voltage-gated Ca<sup>2+</sup> currents. To record  $I_{K(erg)}$ , cells were bathed in high-K<sup>+</sup>, Ca<sup>2+</sup>-free solution which contained (in mM): KCl 130, NaCl 10, MgCl<sub>2</sub> 3, and HEPES 5 adjusted to pH 7.4 with KOH. For the investigations on  $I_{K(erg)}$ ,  $I_h$  or spontaneous action currents (ACs), we backfilled the electrode with the internal solution (in mM): K-aspartate 130, KCl 20, KH<sub>2</sub>PO<sub>4</sub> 1, MgCl<sub>2</sub> 1, EGTA 0.1, Na<sub>2</sub>ATP 3, Na<sub>2</sub>GTP 0.1, and HEPES 5 adjusted to pH 7.2 with KOH, while to measure  $I_{Na}$  and to minimize contamination of K<sup>+</sup> currents, K<sup>+</sup> ions in the backfilling solution were substituted for Cs<sup>+</sup> ions, and pH value was titrated to pH 7.2 with CsOH. All solutions were prepared using demineralized water from a Milli-Q water purification system (Merck, Ltd., Taipei, Taiwan). On the day of experiments, we filtered the bathing or backfilling solution and culture medium by using an Acrodisc® syringe filter with a 0.2- $\mu$ m Supor® membrane (Bio-Check; New Taipei City, Taiwan).

#### 4.2. Cell Preparations

GH<sub>3</sub>, originally acquired from the Bioresources Collection and Research Center ([BCRC-60015]; Hsinchu, Taiwan), were grown in Ham's F-12 medium supplemented with 15% (by volume) horse serum, 2.5% (by volume) fetal calf serum and 2 mM L-glutamine. The rat INS-1 cell line (clone 832/13) was kindly provided by Dr. Christopher B. Newgard, Duke University, Durham, NC, USA. INS-1 cells were cultured in RPMI-1460 medium with 11.1 mM D-glucose which was supplemented with 10% (by volume) fetal bovine serum, 10 mM HEPES, 2 mM L-glutamine, 1 mM sodium pyruvate, and 50 μM β-mercaptoethanol [35,42,51]. GH<sub>3</sub> or INS-1 cells were maintained at 37 °C in a 95% air and 5% CO<sub>2</sub> humidified atmosphere. The viability of these cells was quantified by the trypan blue dye-exclusion method. The electrophysiological recordings were undertaken five or six days after cells had been cultured up to 60–80% confluence.

#### 4.3. Electrophysiological Measurements

Prior to measurements, GH<sub>3</sub> or INS-1 cells were harvested with 1% trypsin/EDTA solution and an aliquot of cell suspension was rapidly transferred to a custom-built recording chamber which was firmly mounted on the stage of an inverted DM-IL microscope (Leica; Major Products, New Taipei City, Taiwan). Cells were bathed at room temperature (20–25 °C) in HEPES-buffered normal Tyrode's solution, the composition of which was detailed above. To prepare patch electrodes from Kimax-51 capillaries (outer diameter of 1.5 to 1.8 mm) (#34500-99; Kimble, Dogger, New Taipei City, Taiwan), we used either a horizontal P-97 Flaming/Brown puller (Sutter; Taiwan Instrument, Tainan, Taiwan) or a vertical PP-830 puller (Narishige; Taiwan Instrument, Tainan, Taiwan), and we then further fire-polished the tip with MF-83 microforge (Narishige). During the recordings, the electrodes, which had the resistance ranging between 3 and 5 MΩ when filled with different internal solution stated above, were tightly mounted to the holder, and they were then maneuvered by using MX-4 manipulator (Narishige) and finely operated by MHW-3 hydraulic micromanipulator (Narishige). We performed the patch-clamp technique with dynamic adaptive suctioning (i.e., decremental change of suction pressure in response to a progressive increase in the electrode resistance) in whole-cell or cell-attached configuration by an Axopatch-200B (Molecular Devices; Advance Biotech, New Taipei City, Taiwan) or RK-400 (Bio-Logic, Claix, France) amplifier [41,52,53]. Liquid junction potentials, which commonly developed at pipette tip when the composition of internal solution was different from that in the bath, were nulled shortly before seal formation was made, and whole-cell data were corrected by such junction potentials.

Action currents (ACs), which corresponds with the occurrence of action potentials detected under whole-cell voltage measurements, were undertaken in cell-attached current recordings [40,53,54]. For AC measurements, the holding voltage was set at the level of the resting potential (~−70 mV). As such, AC measurements were achieved to ensure the quantification of the underlying firing frequency with being void of clear changes in intracellular milieu. The details of data recordings and analyses were listed in the Supplementary Materials.

#### 4.4. Statistical Analyses

Linearized or non-linearized curve-fitting procedure (i.e., least-squares approximation) used in this study was undertaken by using either the SOLVER function (i.e., the generalized reduced gradient method of iteration) embedded in Excel 2016 (Microsoft) or OriginPro 2016 (OriginLab). The experimental results are presented as mean value ± standard error of the mean (SEM) with sample sizes (*n*) indicative of the cell numbers from which the data were collected. Student's *t*-test (paired or unpaired) was initially employed for the statistical analyses. As the statistical difference among different groups was necessarily determined, we performed either analysis of variance (ANOVA)-1 or ANOVA-2 with or without repeated measures followed by Duncan's post hoc test. A *p*-value of < 0.05 was considered to indicate statistical difference.



## 5. Conclusions

Collectively, our findings showed that Gom A can differentially inhibit peak and sustained  $I_{Na}$  in endocrine cells. This would provide important insights into the underlying ionic mechanism for Gom A actions.

**Supplementary Materials:** The following are available online at <http://www.mdpi.com/1422-0067/21/22/8816/s1>.

**Author Contributions:** Conceptualization, W.-T.C. and S.-N.W.; methodology, S.-N.W.; software, S.-N.W.; validation, W.-T.C. and S.-N.W.; formal analysis, S.-N.W.; investigation, W.-T.C. and S.-N.W.; resources, S.-N.W.; data curation, S.-N.W.; writing—original draft preparation, S.-N.W.; writing—review and editing, W.-T.C. and S.-N.W.; project administration, S.-N.W.; funding acquisition, S.-N.W. All authors have read and agreed to the published version of the manuscript.

**Funding:** This work was supported in part by a grant from the Ministry of Sciences and Technology (MOST-108-2314-B-006-094), Taiwan.

**Acknowledgments:** The authors would like to thank Ping-Chung Kuo for the comments in this study. They are also grateful to Zi-Han Kao and Shih-Wei Lee for technical assistances.

**Conflicts of Interest:** The authors declare no conflict of interest, financial or otherwise. The authors are responsible for the content and writing of the paper.

## Abbreviations

AC	action current
ANOVA	analysis of variance
Gom A	gomisin A
$I_h$	hyperpolarization-activated cation current
$I_{K(erg)}$	erg-mediated $K^+$ current
$I_{Na}$	voltage-gated $Na^+$ current
$I_{Na(P)}$	persistent $Na^+$ current
$K_D$	dissociation constant;
$Na_V$ channel	voltage-gated $Na^+$ channel
$t_{inact(S)}$	time constant for slow component of $I_{Na}$ inactivation.

## References

1. Panossian, A.; Wikman, G. Pharmacology of Schisandra chinensis Bail.: An overview of Russian research and uses in medicine. *J. Ethnopharmacol.* **2008**, *118*, 183–212. [[CrossRef](#)] [[PubMed](#)]
2. Wei, B.; Li, Q.; Fan, R.; Su, D.; Chen, X.; Jia, Y.; Bi, K. Determination of monoamine and amino acid neurotransmitters and their metabolites in rat brain samples by UFLC–MS/MS for the study of the sedative-hypnotic effects observed during treatment with *S. chinensis*. *J. Pharm. Biomed. Anal.* **2014**, *88*, 416–422. [[CrossRef](#)]
3. Klimek-Szczykutowicz, M.; Szopa, A.; Blicharska, E.; Dziurka, M.; Komsta, Ł.; Ekiert, H. Bioaccumulation of selected macro- and microelements and their impact on antioxidant properties and accumulation of glucosinolates and phenolic acids in in vitro cultures of *Nasturtium officinale* (watercress) microshoots. *Food Chem.* **2019**, *300*, 125184. [[CrossRef](#)] [[PubMed](#)]
4. Zhang, M.; Xu, L.; Yang, H. Schisandra chinensis Fructus and Its Active Ingredients as Promising Resources for the Treatment of Neurological Diseases. *Int. J. Mol. Sci.* **2018**, *19*, 1970. [[CrossRef](#)] [[PubMed](#)]
5. Zhang, Y.; Lv, X.; Liu, R.; Zhang, M.; Liu, H.; Gao, H.; Zhang, Q.; Xu, H.; Li, Q.; Bi, K. An integrated strategy for ascertaining quality marker of Schisandra chinensis (Turcz.) Baill based on correlation analysis between depression-related monoaminergic metabolites and chemical components profiling. *J. Chromatogr. A* **2019**, *1598*, 122–131. [[CrossRef](#)] [[PubMed](#)]
6. Wang, J.; Jiang, B.; Shan, Y.; Wang, X.; Lv, X.; Mohamed, J.; Li, H.; Wang, C.; Chen, J.; Sun, J.-H. Metabolic mapping of Schisandra chinensis lignans and their metabolites in rats using a metabolomic approach based on HPLC with quadrupole time-of-flight MS/MS spectrometry. *J. Sep. Sci.* **2019**, *43*, 378–388. [[CrossRef](#)]

7. Jeong, H.-J.; Han, N.-R.; Kim, K.-Y.; Choi, I.-S.; Kim, H.-M. Gomisins A decreases the LPS-induced expression of iNOS and COX-2 and activation of RIP2/NF- $\kappa$ B in mouse peritoneal macrophages. *Immunopharmacol. Immunotoxicol.* **2014**, *36*, 195–201. [[CrossRef](#)]
8. Yang, B.; Liu, B.; Liu, Y.; Han, H.; Kuang, H.X. Cognitive enhancement of volatile oil from the stems of *Schisandra chinensis* Baill. in Alzheimer's disease rats. *Can. J. Physiol. Pharmacol.* **2018**, *96*, 550–555. [[CrossRef](#)]
9. Yang, B.-Y.; Tan, J.-Y.; Liu, Y.; Liu, B.; Jin, S.; Guo, H.-W.; Kuang, H. A UPLC-TOF/MS-based metabolomics study of rattan stems of *Schisandra chinensis* effects on Alzheimer's disease rats model. *Biomed. Chromatogr.* **2017**, *32*, e4037. [[CrossRef](#)]
10. Yang, B.; Han, W.; Han, H.; Liu, Y.; Guan, W.; Li, X.-M.; Kuang, H. Effects of Lignans from *Schisandra chinensis* Rattan Stems against A $\beta$ 1-42-Induced Memory Impairment in Rats and Neurotoxicity in Primary Neuronal Cells. *Molecules* **2018**, *23*, 870. [[CrossRef](#)]
11. Ye, B.H.; Lee, S.J.; Choi, Y.W.; Park, S.Y.; Kim, C.D. Preventive effect of gomisins J from *Schisandra chinensis* on angiotensin II-induced hypertension via an increased nitric oxide bioavailability. *Hypertens. Res.* **2014**, *38*, 169–177. [[CrossRef](#)] [[PubMed](#)]
12. Hwang, I.S.; Kim, J.E.; Lee, Y.J.; Kwak, M.H.; Choi, Y.H.; Kang, B.C.; Hong, J.T.; Hwang, D. Protective effects of gomisins A isolated from *Schisandra chinensis* against CCl<sub>4</sub>-induced hepatic and renal injury. *Int. J. Mol. Med.* **2013**, *31*, 888–898. [[CrossRef](#)] [[PubMed](#)]
13. Kim, E.-J.; Jang, M.; Lee, M.J.; Choi, J.H.; Lee, S.J.; Kim, S.K.; Jang, D.S.; Cho, I.-H. *Schisandra chinensis* Stem Ameliorates 3-Nitropropionic Acid-Induced Striatal Toxicity via Activation of the Nrf2 Pathway and Inhibition of the MAPKs and NF- $\kappa$ B Pathways. *Front. Pharmacol.* **2017**, *8*, 673. [[CrossRef](#)] [[PubMed](#)]
14. Nam, S.-Y.; Kim, K.-Y.; Kim, M.H.; Jang, J.-B.; Rah, S.-Y.; Lee, J.-M.; Kim, H.-M.; Jeong, H.-J. Anti-inflammatory effects of a traditional Korean medicine: Ojajeonjonghwan. *Pharm. Biol.* **2017**, *55*, 1856–1862. [[CrossRef](#)]
15. Nam, Y.; Kim, H.J.; Kim, Y.-M.; Chin, Y.-W.; Kim, Y.K.; Bae, H.S.; Nam, J.H.; Kim, W.K. Activation of transient receptor potential vanilloid 3 by the methanolic extract of *Schisandra chinensis* fruit and its chemical constituent  $\gamma$ -schisandrin. *Korean J. Physiol. Pharmacol.* **2017**, *21*, 309–316. [[CrossRef](#)]
16. Takanche, J.S.; Kim, J.-E.; Han, S.-H.; Yi, H.-K. Effect of gomisins A on osteoblast differentiation in high glucose-mediated oxidative stress. *Phytomedicine* **2019**, *66*, 153107. [[CrossRef](#)]
17. Hwang, D.; Shin, S.Y.; Lee, Y.; Hyun, J.; Yong, Y.; Park, J.C.; Lee, Y.H.; Lim, Y. A compound isolated from *Schisandra chinensis* induces apoptosis. *Bioorg. Med. Chem. Lett.* **2011**, *21*, 6054–6057. [[CrossRef](#)]
18. Choi, B.R.; Kim, H.K.; Park, J.K. Effects of *Schisandra chinensis* fruit extract and gomisins A on the contractility of penile corpus cavernosum smooth muscle: A potential mechanism through the nitric oxide-cyclic guanosine monophosphate pathway. *Nutr. Res. Pr.* **2018**, *12*, 291–297. [[CrossRef](#)]
19. Yang, J.; Ip, P.S.; Yeung, J.H.; Che, C.-T. Inhibitory effect of schisandrin on spontaneous contraction of isolated rat colon. *Phytomedicine* **2011**, *18*, 998–1005. [[CrossRef](#)]
20. Panossian, A.; Wagner, H. Stimulating effect of adaptogens: An overview with particular reference to their efficacy following single dose administration. *Phytother. Res.* **2005**, *19*, 819–838. [[CrossRef](#)]
21. Li, J.; Wang, J.; Shao, J.-Q.; Du, H.; Wang, Y.-T.; Peng, L. Effect of *Schisandra chinensis* on interleukins, glucose metabolism, and pituitary-adrenal and gonadal axis in rats under strenuous swimming exercise. *Chin. J. Integr. Med.* **2014**, *21*, 43–48. [[CrossRef](#)] [[PubMed](#)]
22. Giridharan, V.V.; Thandavarayan, R.A.; Sato, S.; Ko, K.M.; Konishi, T. Prevention of scopolamine-induced memory deficits by schisandrin B, an antioxidant lignan from *Schisandra chinensis* in mice. *Free. Radic. Res.* **2011**, *45*, 950–958. [[CrossRef](#)] [[PubMed](#)]
23. Hsu, Y.-S.; Kuo, Y.-H.; Cheng, H.-L.; Flatt, P.R.; Liu, H.-K. *Schisandra arisanensis* extract attenuates cytokine-mediated cytotoxicity in insulin-secreting cells. *World J. Gastroenterol.* **2012**, *18*, 6809–6818. [[CrossRef](#)] [[PubMed](#)]
24. Jeong, E.J.; Lee, H.K.; Lee, K.Y.; Jeon, B.J.; Kim, D.H.; Park, J.-H.; Song, J.-H.; Huh, J.; Lee, J.-H.; Sung, S.H. The effects of lignan-riched extract of *Schisandra chinensis* on amyloid- $\beta$ -induced cognitive impairment and neurotoxicity in the cortex and hippocampus of mouse. *J. Ethnopharmacol.* **2013**, *146*, 347–354. [[CrossRef](#)]
25. An, L.; Wang, Y.; Wang, C.; Fan, M.; Han, X.; Xu, G.; Yuan, G.; Li, H.; Sheng, Y.; Wang, M.; et al. Protective effect of *Schisandra chinensis* oil on pancreatic  $\beta$ -cells in diabetic rats. *Endocrine* **2014**, *48*, 818–825. [[CrossRef](#)]
26. Hong, S.-H.; Li, M.; Jeung, E.-B.; Lee, G.-S.; Hong, E.-J.; Choi, Y.-W.; An, B.-S. Therapeutic effects of *Schisandra chinensis* on the hyperprolactinemia in rat. *Int. J. Oncol.* **2017**, *50*, 1448–1454. [[CrossRef](#)]

27. Catterall, W.A.; Goldin, A.L.; Waxman, S.G. International Union of Pharmacology. XLVII. Nomenclature and Structure-Function Relationships of Voltage-Gated Sodium Channels. *Pharmacol. Rev.* **2005**, *57*, 397–409. [[CrossRef](#)]
28. Stojilkovic, S.S.; Tabak, J.; Bertram, R. Ion Channels and Signaling in the Pituitary Gland. *Endocr. Rev.* **2010**, *31*, 845–915. [[CrossRef](#)]
29. Chen, B.-S.; Lo, Y.-C.; Peng, H.; Hsu, T.-I.; Wu, S.-N. Effects of Ranolazine, a Novel Anti-anginal Drug, on Ion Currents and Membrane Potential in Pituitary Tumor GH3 Cells and NG108-15 Neuronal Cells. *J. Pharmacol. Sci.* **2009**, *110*, 295–305. [[CrossRef](#)]
30. Lai, M.-C.; Tzeng, R.-C.; Huang, C.-W.; Wu, S.-N. The Novel Direct Modulatory Effects of Perampanel, an Antagonist of AMPA Receptors, on Voltage-Gated Sodium and M-type Potassium Currents. *Biomolecules* **2019**, *9*, 638. [[CrossRef](#)]
31. Anderson, L.L.; Thompson, C.H.; Hawkins, N.A.; Nath, R.D.; Petersohn, A.A.; Rajamani, S.; Bush, W.S.; Frankel, W.N.; Vanoye, C.G.; Kearney, J.A.; et al. Antiepileptic activity of preferential inhibitors of persistent sodium current. *Epilepsia* **2014**, *55*, 1274–1283. [[CrossRef](#)] [[PubMed](#)]
32. Niu, X.Y.; Wang, W.J.; Bian, Z.J.; Ren, Z.H. Effects of schizandrol on the central nervous system. *Yao Xue Xue Bao* **1983**, *18*, 638. [[CrossRef](#)]
33. Chang, W.-T.; Wu, S.-N. Activation of voltage-gated sodium current and inhibition of erg-mediated potassium current caused by telmisartan, an antagonist of angiotensin II type-1 receptor, in HL-1 atrial cardiomyocytes. *Clin. Exp. Pharmacol. Physiol.* **2018**, *45*, 797–807. [[CrossRef](#)] [[PubMed](#)]
34. Lee, S.B.; Noh, S.; Yeom, H.D.; Jo, H.; Eom, S.; Kim, Y.S.; Nam, S.; Bae, H.; Lee, J.-H. A Molecular Basis for the Inhibition of Transient Receptor Potential Vanilloid Type 1 by Gomisin A. *Evid.-Based Complement. Altern. Med.* **2017**, *2017*, 6945912. [[CrossRef](#)] [[PubMed](#)]
35. Kuo, P.-C.; Kao, Z.-H.; Lee, S.-W.; Wu, S.-N. Effects of Sesamin, the Major Furofuran Lignan of Sesame Oil, on the Amplitude and Gating of Voltage-Gated Na(+) and K(+) Currents. *Molecules* **2020**, *25*, 3062. [[CrossRef](#)]
36. Kubica, P.; Szopa, A.; Ekiert, H. Production of verbascoside and phenolic acids in biomass of *Verbena officinalis* L. (vervain) cultured under different in vitro conditions. *Nat. Prod. Res.* **2017**, *31*, 1663–1668. [[CrossRef](#)]
37. Wu, S.-N.; Chen, B.-S.; Hsu, T.-I.; Peng, H.; Wu, Y.-H.; Lo, Y.-C. Analytical studies of rapidly inactivating and noninactivating sodium currents in differentiated NG108-15 neuronal cells. *J. Theor. Biol.* **2009**, *259*, 828–836. [[CrossRef](#)]
38. Tabarean, I.V.; Narahashi, T. Kinetics of modulation of tetrodotoxin-sensitive and tetrodotoxin-resistant sodium channels by tetramethrin and deltamethrin. *J. Pharmacol. Exp. Ther.* **2001**, *299*, 988–997.
39. So, E.C.; Wu, S.-N.; Lo, Y.-C.; Su, K. Differential regulation of tefluthrin and telmisartan on the gating charges of I Na activation and inactivation as well as on resurgent and persistent I Na in a pituitary cell line (GH 3). *Toxicol. Lett.* **2018**, *285*, 104–112. [[CrossRef](#)]
40. Hsu, H.-T.; Lo, Y.-C.; Wu, S.-N. Characterization of Convergent Suppression by UCL-2077 (3-(Triphenylmethylaminomethyl)pyridine), Known to Inhibit Slow Afterhyperpolarization, of erg-Mediated Potassium Currents and Intermediate-Conductance Calcium-Activated Potassium Channels. *Int. J. Mol. Sci.* **2020**, *21*, 1441. [[CrossRef](#)]
41. Chang, W.; Gao, Z.-H.; Lo, Y.-C.; Wu, S.-N. Evidence for Effective Inhibitory Actions on Hyperpolarization-Activated Cation Current Caused by Ganoderma Triterpenoids, the Main Active Constituents of Ganoderma Spores. *Molecules* **2019**, *24*, 4256. [[CrossRef](#)] [[PubMed](#)]
42. Kuo, P.-C.; Liu, Y.; Lo, Y.-C.; Wu, S.-N. Characterization of Inhibitory Effectiveness in Hyperpolarization-Activated Cation Currents by a Group of ent-Kaurane-Type Diterpenoids from *Croton tonkinensis*. *Int. J. Mol. Sci.* **2020**, *21*, 1268. [[CrossRef](#)] [[PubMed](#)]
43. Kwon, D.Y.; Kim, D.S.; Yang, H.J.; Park, S. The lignan-rich fractions of *Fructus Schisandrae* improve insulin sensitivity via the PPAR- $\gamma$  pathways in in vitro and in vivo studies. *J. Ethnopharmacol.* **2011**, *135*, 455–462. [[CrossRef](#)] [[PubMed](#)]
44. Lisi, D.; Andrews, E.; Parry, C.; Hill, C.; Ombengi, D.; Ling, H. The Effect of Ranolazine on Glycemic Control: A Narrative Review to Define the Target Population. *Cardiovasc. Drugs Ther.* **2019**, *33*, 755–761. [[CrossRef](#)] [[PubMed](#)]
45. Zhang, Y.; Lv, X.; Qu, J.; Zhang, X.; Zhang, M.; Gao, H.; Zhang, Q.; Liu, R.; Xu, H.; Li, Q.; et al. A systematic strategy for screening therapeutic constituents of *Schisandra chinensis* (Turcz.) Baill infiltrated blood-brain barrier oriented in lesions using ethanol and water extracts: A novel perspective for exploring chemical material basis of herb medicines. *Acta Pharm. Sin. B* **2020**, *10*, 557–568. [[CrossRef](#)]

46. Zhai, J.; Zhang, F.; Gao, S.; Chen, L.; Feng, G.; Yin, J.; Chen, W. Time- and NADPH-Dependent Inhibition on CYP3A by Gomisins A and the Pharmacokinetic Interactions between Gomisins A and Cyclophosphamide in Rats. *Molecules* **2017**, *22*, 1298. [[CrossRef](#)]
47. Pan, Y.; Cummins, T.R. Distinct functional alterations in SCN8A epilepsy mutant channels. *J. Physiol.* **2020**, *598*, 381–401. [[CrossRef](#)]
48. Rajamani, S.; Shryock, J.C.; Belardinelli, L. Rapid Kinetic Interactions of Ranolazine With HERG K<sup>+</sup> Current. *J. Cardiovasc. Pharmacol.* **2008**, *51*, 581–589. [[CrossRef](#)]
49. Rizzetto, R.; Rocchetti, M.; Sala, L.; Ronchi, C.; Villa, A.; Ferrandi, M.; Molinari, I.; Bertuzzi, F.; Zaza, A. Late sodium current (I<sub>NaL</sub>) in pancreatic  $\beta$ -cells. *Pflügers Archiv-Eur. J. Physiol.* **2015**, *467*, 1757–1768. [[CrossRef](#)]
50. Armstrong, C.M. Na channel inactivation from open and closed states. *Proc. Natl. Acad. Sci. USA* **2006**, *103*, 17991–17996. [[CrossRef](#)]
51. Kuo, P.-C.; Yang, C.-J.; Lee, Y.-C.; Chen, P.-C.; Liu, Y.-C.; Wu, S.-N. The comprehensive electrophysiological study of curcuminoids on delayed-rectifier K<sup>(+)</sup> currents in insulin-secreting cells. *Eur. J. Pharmacol.* **2018**, *819*, 233–241. [[CrossRef](#)] [[PubMed](#)]
52. McBride, D.W., Jr.; Hamill, O.P. Simplified fast pressure-clamp technique for studying mechanically gated channels. *Methods Enzymol.* **1999**, *294*, 482–489. [[CrossRef](#)] [[PubMed](#)]
53. Wu, S.-N.; Wu, Y.-H.; Chen, B.-S.; Lo, Y.-C.; Liu, Y.-C. Underlying mechanism of actions of tefluthrin, a pyrethroid insecticide, on voltage-gated ion currents and on action currents in pituitary tumor (GH3) cells and GnRH-secreting (GT1-7) neurons. *Toxicology* **2009**, *258*, 70–77. [[CrossRef](#)] [[PubMed](#)]
54. Lo, Y.-C.; Tseng, Y.-T.; Liu, C.-M.; Wu, B.-N.; Wu, S.-N. Actions of KMUP-1, a xanthine and piperazine derivative, on voltage-gated Na<sup>(+)</sup> and Ca<sup>(2+)</sup>-activated K<sup>(+)</sup> currents in GH3 pituitary tumour cells. *Br. J. Pharmacol.* **2015**, *172*, 5110–5122. [[CrossRef](#)] [[PubMed](#)]

**Publisher's Note:** MDPI stays neutral with regard to jurisdictional claims in published maps and institutional affiliations.



© 2020 by the authors. Licensee MDPI, Basel, Switzerland. This article is an open access article distributed under the terms and conditions of the Creative Commons Attribution (CC BY) license (<http://creativecommons.org/licenses/by/4.0/>).